УДК 546.27:547.914

Х.Х. КУЄН,
Університет Науки і Технологій,
Да Нанг 550000, В'єтнам
e-mail: hhquyen@dut.udn.vn

Х.М. НГУЄН,
Університет Нотр-Дам, кафедра аерокосмічної та машинобудівної інженерії,
Нотр-Дам, Індіана 46556, США
e-mail: hnguye28@nd.edu

В.Ч.М. ТРАН,
Університет Науки і Технологій,
Да Нанг 550000, В'єтнам

Ф.Ц. ЛЕ,
Університет Науки і Технологій,
Да Нанг 550000, В'єтнам

М. КУРАШІНА,
Університет Токусіма, кафедра прикладної хімії, Вища школа науки і технологій,
Токусіма 770-8506, Японія

М. ЯСУДЗАВА,
Університет Токусіма, кафедра прикладної хімії, Вища школа науки і технологій,
Токусіма 770-8506, Японія

УДОСКОНАЛЕННЯ МЕТОДУ ВИДАЛЕННЯ БОРУ З ВОДНИХ РОЗЧИНІВ ЗА ДОПОМОГОЮ СМОЛИ AMBERLITE IRA 743: РОЛЬ РН ТА АКТИВАЦІЇ СМОЛИ[1]

Зниження підвищеного рівня бору у водних екосистемах є важливим через його токсичність для людини та рослин. Досліджено використання активованої смоли Amberlite IRA 743 для видалення бору з водних розчинів. В експериментальних умовах вивчали вплив pH, початкової концентрації бору, часу контакту та іонної сили на адсорбцію бору активованою смолою. Активація з використанням 0.1 M HCl та 0.1 M NaOH значно підвищувала її адсорбційну здатність. Поглинання бору збільшувалось зі зростанням pH, досягаючи піку при pH 8. Ізотерма Ленгмюра добре узгоджується з отриманими даними, з максимальною ємністю 6.39 мг/г для необробленої та 9.75 мг/г для активованої смоли. Кінетика відповідала моделям псевдо-першого та другого порядку, досягаючи рівноваги через 12 год. Додавання NaCl та KCl мало не-

[1]This research is funded by the Ministry of Education and Training of Vietnam (Project No: B2023.DNA.09).

Цитування: Куєн Х.Х., Нгуєн Х.М., Тран В.Ч.М., Ле Ф.Ц., Курашіна М., Ясудзава М. Удосконалення методу видалення бору з водних розчинів за допомогою смоли AMBERLITE IRA 743: роль pH та активації смоли. *Гідробіол. журн.* 2025. Т. 61, № 6. С. 97—115.

значний вплив, тоді як $CaCl_2$ та $MgCl_2$ сприяли видаленню бора. Використання активованої смоли для видалення бору зі стічних вод від десульфуризації димових газів досягало ефективності до 93.2 %. Отримані результати свідчать про те, що активована смола Amberlite IRA 743 є перспективним адсорбентом для видалення бору з забрудненої води.

***Ключові слова**: смола Amberlite IRA 743, видалення бору, адсорбція, активація, кінетика адсорбції.*

Introduction

Water pollution represents a critical worldwide challenge that endangers human health and ecological systems [6]. Boron and its compounds naturally occur in aquatic ecosystems in forms such as borosilicate minerals, boric acid, and borate salts [21, 28]. However, the predominant source of boron contamination in water systems arises from industrial effluents, encompassing sectors such as ceramics, glass manufacturing, textiles, metallurgy, nuclear energy, cleaning, wood preservation, agriculture, and healthcare [1, 19, 25]. Furthermore, coal combustion byproducts from coal-fired power plants, including fly ash, bottom ash, boiler slag, and scrubber sludge, are often stored in landfills and lagoons [10, 34]. During coal combustion, boron oxides such as BO_2, B_2O_2, and B_2O_3 are formed. Through subsequent processes, including wet flue gas desulfurization, these oxides are converted to boric acid (H_3BO_3) via hydration and dissociation reactions [23]. A considerable proportion of boron from coal combustion byproducts exists in soluble forms, allowing it to leach into groundwater and surface waters, thus posing a significant environmental threat [22].

Boron is a crucial micronutrient for plant growth, involved in the metabolism of nucleic acids, carbohydrates, nitrogen, and phenolic compounds. In addition, the role of boron in critical processes such as pollen tube formation, photosynthesis, and enzyme interaction is well-documented, contributing to crop and fruit yield [35]. However, excessive boron concentrations can lead to toxicity. Notably, plant species such as lemon and blackberry exhibit heightened sensitivity to boron concentrations exceeding 0.5 mg/L [5]. Moreover, prolonged exposure to elevated boron levels in drinking water and food sources can disrupt human physiological systems, impacting the cardiovascular, nervous, digestive, reproductive, renal, and endocrine systems [17, 37]. The World Health Organization (WHO) has set a recommended boron concentration limit of 2.4 mg/L in drinking water, with more stringent standards of 1.0 mg/L in regions such as the European Union, the United Kingdom, South Korea, Singapore, and Japan [33]. In the United States, the allowable concentration is regulated between 0.6 and 1.0 mg/L [41]. Consequently, efficient boron removal from water sources is imperative for safeguarding public health and maintaining environmental integrity.

Various techniques have been developed for boron removal from aqueous solutions, including chemical oxo-precipitation [20], adsorption [36], nanofiltration [7], reverse osmosis [38], membrane filtration [16], electrocoagulation [39], and electrodialysis [12]. Among these, ion exchange stands out due to its

exceptional efficiency, operational flexibility, and absence of chemical byproducts [3]. Commercial chelating resins such as Amberlite IRA 743 and Diaion CR05, which contain functional groups with hydroxyl groups in cis position (*vis*-diols), are particularly effective for boron complexation [4]. These resins exhibit a strong affinity for boron, forming stable complexes due to their high selectivity and minimal reactivity with other elements [32]. Amberlite IRA 743, for instance, has become widely utilized for the selective removal and recovery of boron from aqueous systems [18]. This resin consists of a macroporous polystyrene matrix crosslinked with divinylbenzene and functionalized with N-methyl-D-glucamine (NMDG) groups containing *vis*-diols [24]. The boron removal efficiency of Amberlite IRA 743 has been reported to vary substantially, with reported efficiencies ranging from 10 to 99 % [27]. This variability is influenced by several factors, including resin particle size, contact time, pH, temperature, and the presence of competing ions. Among these, the pH of the boron solution has garnered particular attention due to its significant impact on the boron adsorption efficiency of resin.

This work aims to assess the boron adsorption performance of activated Amberlite IRA 743 resin as an adsorbent in boron removal from aqueous solution. Activated Amberlite IRA 743 resins were prepared for boron removal by immersing acidic and alkaline solutions. Batch experiments were conducted to evaluate the impacts of different experimental parameters, including pH, initial concentration, contact time, and ionic strength with various chloride salts such as NaCl, KCl, $CaCl_2$, and $MgCl_2$, on boron removal of both Amberlite IRA 743 resin and activated Amberlite IRA 743 resin. Furthermore, the potential boron adsorption mechanism was discussed. The regeneration of adsorbents and the boron removal capacity from wastewater of both resins were also investigated. These findings provide insights into the resin's adsorption behavior, which may support future investigations into its potential application in large-scale boron removal systems, particularly for industrial wastewater treatment contexts such as flue gas desulfurization effluents.

Material and Methods

Amberlite IRA 743 resin (particle size 500—700 μm, water retention capacity — 48—54 %) was obtained from the Dow Chemical Company, the US. Sodium hydroxide (NaOH, purity >97 %) and hydrochloric acid (HCl, purity >35~37 %) used for the pH adjustment, boron standard solution (1000 mg/L for chemical analysis), and boric acid (H_3BO_3, purity >99.5 %) were purchased from Kanto, Japan. All materials are commercially available and used without further purification.

In the previous study, crosslinked gluconated chitosan particles/beads containing vis-diol after boron adsorption were treated in 0.1M HCl solution, then activated using a 0.1M NaOH solution for regeneration and reusability of adsorbents [31]. Based on this concept, to improve the capacity for boron removal, 4 g of Amberlite IRA 743 resin was introduced to 50 mL of Mili-Q water for 5 h under magnetic stirring conditions. Following this, this resin was immersed in i, 50 mL of 0.1 M HCl solution for 1 h with magnetic stirring, then

was rinsed thoroughly with Mili-Q water (Amberlite IRA 743 resin-AT) or ii, 50 mL of 0.1 M HCl solution for 1 h with magnetic stirring, followed by treatment in 50 mL of 0.1 M NaOH solution for 1 h with magnetic stirring, then was washed thoroughly with Mili-Q water (Amberlite IRA 743 resin-AAT). Afterwards, both resins were dried in a clean bench for further investigation. The preparation of Amberlite IRA 743 resin-AT and Amberlite IRA 743 resin-AAT is shown in **Fig. 1.**

The study of pH impact on boron adsorption capacity was conducted by adding 0.8 g of Amberlite IRA 743 resin or activated Amberlite IRA 743 resin to 20 mL of boric acid solution with the initial boron concentration of 400 mg/L. The initial pH of the boron solution was adjusted to 5.6, 6.9. 7.9, 9.2, 9.9, 10.7, and 12.2 by using 0.1 M NaOH solution. The pH value was determined by using a pH meter (F-52, Horiba, Japan). After shaking at 25 °C for 24 h, the filtrate was collected by filtration using Whatman 50 filter paper (2.7 μm particle retention).

For the study of adsorption isotherms, 8 g of Amberlite IRA 743 resin or activated Amberlite IRA 743 resin was added to the boric acid solution with the boron initial concentration ranging from 10 to 400 mg/L in a shaker at 25 °C for 24 h. The initial pH solution was controlled at the optimal pH value, according to the previous experiment on the pH effect.

Langmuir, Freundlich, and Temkin models were used to describe the experimental adsorption isotherm data. The Langmuir, Freundlich, and Temkin isotherms are given by the following equations, respectively:

$$q_e = \frac{bq_{\max}C_e}{1+bC_e} \quad (1)$$

$$q_e = K_F C_e^{1/n} \quad (2)$$

$$q_e = B\ln(A_T C_e) \quad (3)$$

$$B = RT/b_T \quad (4)$$

where q_e is the amount of boron adsorbed per gram of resin at equilibrium (mg/g), q_{max} is the maximum adsorption capacity of resin (mg/g), and C_e is the concentration of boron at equilibrium in solution (mg/L). In the Langmuir model (Eq. 1), b is related to the energy of adsorption (L/mg resin). In the Freundlich model (Eq. 2), K_F and n are the Freundlich adsorption constants, indicating the relative capacity and the adsorption intensity, respectively. In the Temkin model (Eq. 3 and Eq. 4), R is the ideal gas constant (8.3145 J/mol K), T is thermodynamic temperature (K), b_T is the constant of Temkin isotherm (kJ g/mol^2), and A_T is related to the equilibrium binding constant, which is associated with the maximum binding energy (L/g).

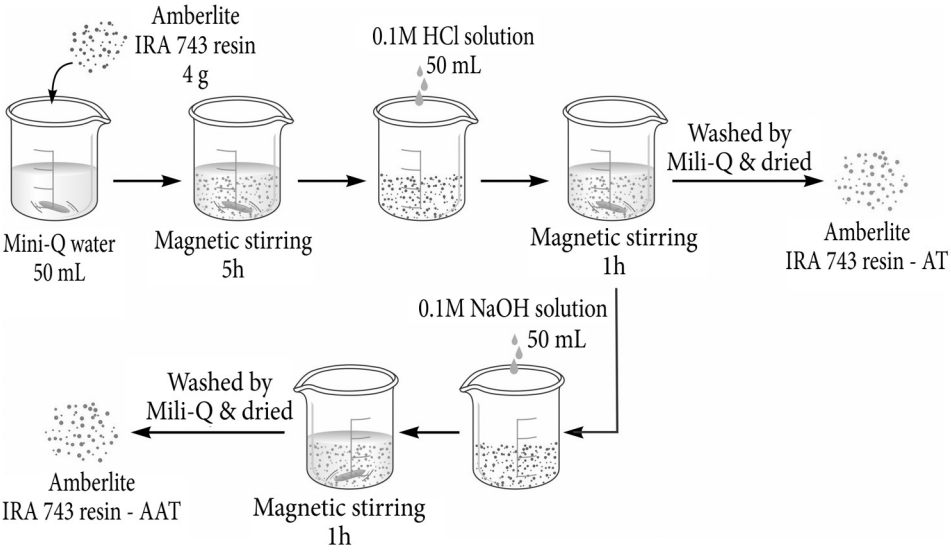

Fig. 1. Schematic diagram of the Amberlite IRA 743 resin activation experiment

For the adsorption kinetic experiment, 0.8 g of Amberlite IRA 743 resin or activated Amberlite IRA 743 resin was added to the boric acid solution with the boron initial concentration of 400 mg/L in a shaker at 25 °C for different times from 15 min to 24 h. The initial pH solution was adjusted to the optimal pH value, following the previous pH effect experiment.

Different models, such as the pseudo-first order, pseudo-second order, and intra-particle diffusion, were applied to simulate boron adsorption kinetics. All models are presented as follows:

$$\log(q_e - q_t) = \log(q_e) - \frac{k_1 t}{2.303} \tag{5}$$

$$\frac{t}{q_t} = \frac{1}{k_2 q_e^2} + \frac{t}{q_e} \tag{6}$$

$$q_t = K_{diff}\, t^{1/2} + C \tag{7}$$

where q_e and q_t (mg/g) are the adsorbed amount at equilibrium and at time t (min). k_1 (min^{-1}) is the rate constant of pseudo-first order model. k_2 (g mg^{-1} min^{-1}) represents the rate constant of the pseudo-second order model. K_{diff} (mg g^{-1} $min^{-1/2}$) is the diffusion rate constant, and C (mg g^{-1} mg/g) is intra-particle diffusion constant intercept of the line.

For the study of ionic strength effect, 0.8 g of Amberlite IRA 743 resin or activated Amberlite IRA 743 resin was added to 20 mL of the boric acid solution with an initial boron concentration of 400 mg/L in the presence of different chloride salts, including NaCl, KCl, $CaCl_2$, or $MgCl_2$. The ion strengths were

adjusted to 1.0, 2.0, 3.0, and 4.0 mol/L for Na^+, K^+, and Ca^{2+}, and 0.5, 1.0, 1.5, and 2.0 mol/L for Mg^{2+}, respectively. All samples were shaken at 25 °C for 24 h. At the end of the experiment, filtrate was obtained through filtration for the determination of boron concentrations.

For the regeneration experiment, adsorbents collected from the boron adsorption process were rinsed several times with Mili-Q water. Following this, the adsorbents were placed in a polypropylene bottle with 50 mL of a 0.1 M HCl solution and agitated at 25 °C for 24 h. After this treatment, the adsorbents were washed several times with Mili-Q water, then immersed in 50 mL of a 0.1 M NaOH solution and agitated at 25 °C for 12 h. Finally, the adsorbents were dried in a clean bench for the subsequent adsorption-desorption cycle.

Blank samples were also performed for each batch test. The boron concentration before and after filtration was analyzed with UV/VIS/NIR Spectrophotometer by Azomethine-H method at the wavelength of 415 nm. The instrumental limit of detection (LOD) and limit of quantification (LOQ) for this analysis is 0.02 and 0.5 ppm [30]. The removal efficiency of boron (H) and capacity of boron adsorption (q_e) were calculated using the following equations:

$$H = \frac{C_0 - C_e}{C_0} \cdot 100 \quad (8)$$

$$q_e = \frac{C_0 - C_e}{M} \cdot V \quad (9)$$

where C_0 and C_e (mg/L) are the initial and equilibrium boron concentrations, respectively, M (g) is the weight of resin, and V (L) is the boron solution volume.

All adsorption experiments were carried out at least in triplicate.

Results and Discussion

The adsorption performance of various Amberlite IRA 743 resins was examined to explore the feasibility of these resins in diverse pretreatment processes, thereby enhancing their applicability in practice and meeting the requirements of the boron standard. In this experiment, 0.8 g of each resin was added to 20 mL of boric acid solution as an initial boron concentration of 400 mg/L with a pH value of 8.05. The boron removal efficiency and boron adsorption capacity of various resins are presented in **Fig. 2.** The maximum boron adsorption capacity of Amberlite IRA 743 resin-AAT was 8.55 mg/g. In contrast, those of Amberlite IRA 743 resin and Amberlite IRA 743 resin-AT were 6.20 and 4.53 mg/g, respectively. For boron removal efficiency, Amberlite IRA 743 resin-AAT reached 82.8 %, compared to 60.4 % and 43.7 % for Amberlite IRA 743 resin and Amberlite IRA 743 resin-AT. The generation of stable complexes between boron ions and hydroxyl groups relates to the growth of a negative charge on the resin surface. The increase in boron adsorption capacity can be attributed to the enhancement of the negative charge on the surface areas of the resin in the alkaline environment [11]. Consequently, the Amberlite IRA 743

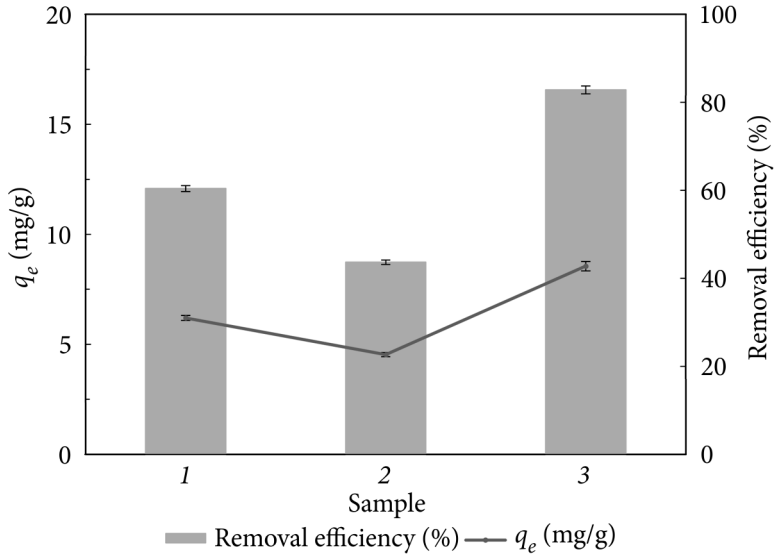

Fig. 2. Boron removal efficiency and boron adsorption capacity of various Amberlite IRA 743 resins: *1* — Amberlite IRA 743 resin; *2* — Amberlite IRA 743 resin-AT; *3* — Amberlite IRA 743 resin-AAT (initial pH — 8.05, initial boron concentration — 400 mg/L, resin dosage — 0.8 g, solution volume — 20 mL, contact time — 24 h, temperature — 25 °C)

resin that was prepared in the acid condition and then in the alkaline condition is deemed appropriate for boron removal in the aqueous media.

The influence of initial pH on the boron adsorption capacity was examined through batch experiments at a controlled pH with initial pH values ranging from 5.6 to 12.2. As depicted in **Fig. 3**, the boron adsorption capacity of Amberlite IRA 743 resin and Amberlite IRA 743 resin-AAT presented a significant enhancement with the elevation of pH from 5.6 to 7.9. The peak boron adsorption capacity of Amberlite IRA 743 resin and Amberlite IRA 743 resin-AAT was recorded at 6.16 mg/g and 8.21 mg/g at the pH of 7.9. In contrast, the boron adsorption capacity decreased when the pH was higher than 7.9. The pH-dependent behaviour of boron adsorption is based on the different forms of boron species and the formation mechanism of borate complexes, which are the products of the interaction between boron species and the NMDG functional groups of the resin. Boric acid $[B(OH)_3]^0$ is regarded as a weak Lewis acid and dissociates to tetrahydroxyborate $[B(OH)_4]^-$ ions by accepting hydroxyl ions through the hydrolysis process under slightly alkaline environments [29]. It has been previously demonstrated that the *vis*-diols of Amberlite IRA 743 resin exhibit a greater affinity for $[B(OH)_4]^-$ species in comparison to $[B(OH)_3]^0$ ions [8]. The observed reduction in boron adsorption capacity at pH levels exceeding 7.9 may be attributed to the predominance of (OH^-) ions, which are likely to engage in competitive interactions with $[B(OH)_4]^-$ for the available sorption sites, consequently diminishing the favorability of the adsorption process for

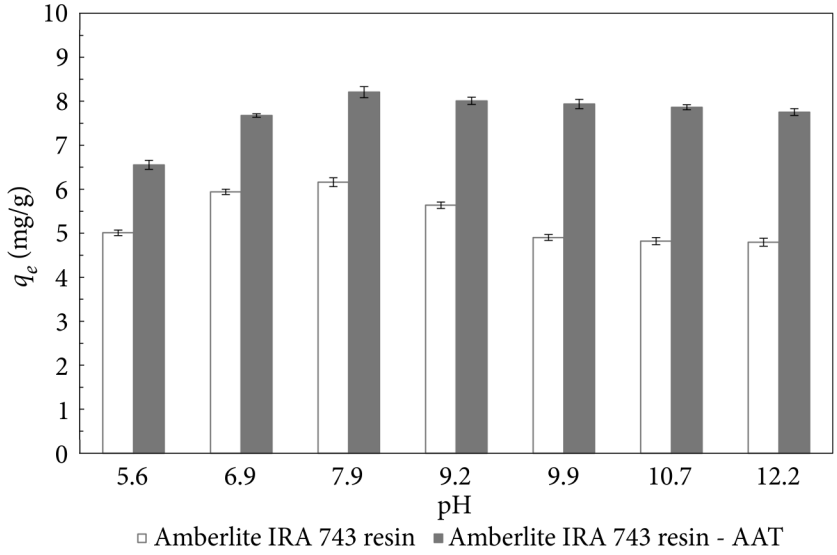

Fig. 3. Boron adsorption capacity of Amberlite IRA 743 resin and Amberlite IRA 743 resin-AAT as a function of pH (initial pH — 5.6—12.2, initial boron concentration — 400 mg/L, resin dosage — 0.8 g, solution volume — 20 mL, contact time — 24 h, temperature — 25 °C)

the $[B(OH)_4]^-$ ions [26]. Furthermore, similar findings have been reported in previous studies [15]. Therefore, pH of 8 was chosen for further experiments.

The boron adsorption isotherm was investigated at different initial concentrations from 10 to 400 mg/L. Isotherm model fittings for Amberlite IRA 743 resin-AAT and Amberlite IRA 743 resin are presented in **Fig. 4**, and fitting parameters are detailed in Table 1. Upon comparing the fitting outcomes of the Langmuir, Freundlich and Temkin isotherm model and the obtained correlation coefficients, it was observed that the R^2 values of the Langmuir isotherm models for both Amberlite IRA 743 resin-AAT and Amberlite IRA 743 resin surpassed those of Freundlich and Temkin isotherm models. This result strongly suggests that the Langmuir isotherm model provided a more accurate depiction of the boron adsorption process. These findings demonstrated that the resins exhibited monolayer adsorption surfaces with all adsorption sites possessing uniform adsorption affinity [14]. The highest adsorption capacity of Amberlite IRA 743 resin-AAT made up 9.75 mg/g, was 1.5 times higher than Amberlite IRA 743 resin for boron removal, which was 6.39 mg/g. This confirms the effectiveness of resin treatment for enhancing boron adsorption capacity. Table 2 shows the comparison of boron adsorption capacity for Amberlite IRA 743 resin-AAT and Amberlite IRA 743 resin with various adsorbents. The data confirmed the efficiency and promising adsorption of Amberlite IRA 743 resin-AAT for boron removal from aqueous solution compared with other adsorbents.

The kinetics of boron adsorption have been examined by determining the required contact time for the adsorption process to achieve equilibrium. As il-

Table 1

Fitting parameters of Langmuir, Freundlich and Temkin isotherm models for boron adsorption using Amberlite IRA 743 resin-AAT and Amberlite IRA 743 resin

Adsorbent	Langmuir model			Freundlich model			Temkin model		
	q_{max} (mg/g)	b (L/mg)	R^2	K_F	n	R^2	B (J/mol)	A_T (L/g)	R^2
Amberlite IRA 743 resin	6.39± 0.099	0.151	0.9996	1.813	3.923	0.9107	0.8515	8.973	0.9374
Amberlite IRA 743 resin-AAT	9.75± 0.137	0.060	0.9998	3.076	4.289	0.8521	0.9682	52.971	0.9857

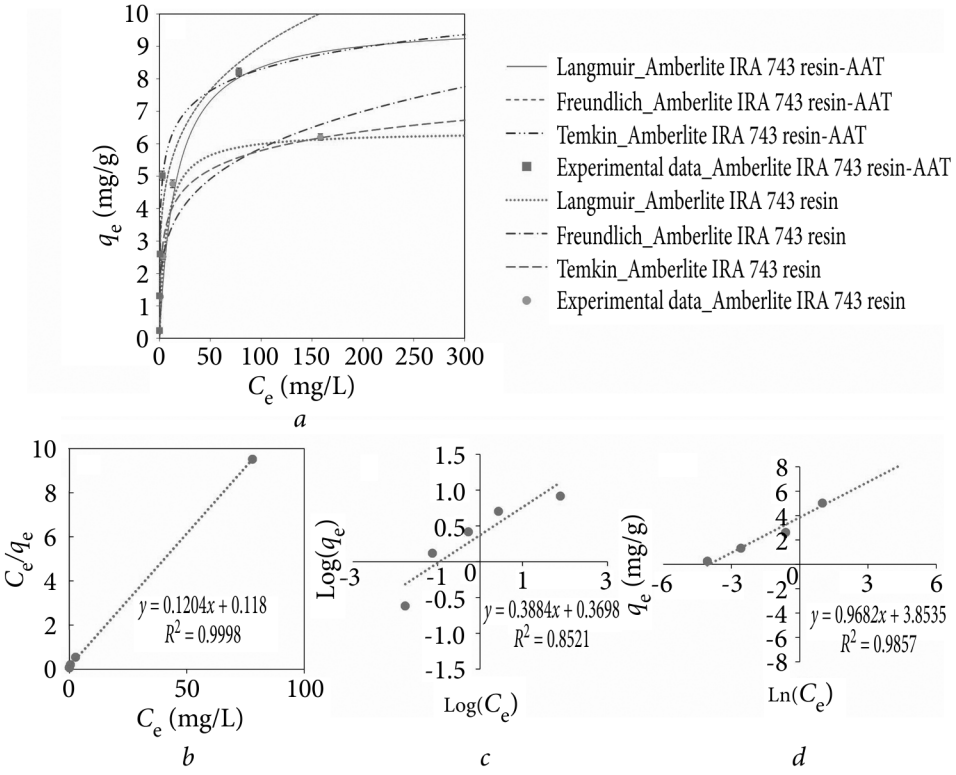

Fig. 4. Langmuir, Freundlich and Temkin isotherm models fitting of boron adsorption onto Amberlite IRA 743 resin-AAT and Amberlite IRA 743 resin (*a*); Linear Langmuir model of Amberlite IRA 743 resin-AAT (*b*); Linear Freundlich model of Amberlite IRA 743 resin-AAT (*c*); Linear Temkin model of Amberlite IRA 743 resin-AAT (*d*) (initial pH — 8.02, initial boron concentration — 10—400 mg/L, resin dosage — 0.8 g, solution volume — 20 mL, contact time — 15 min to 24 h, and temperature — 25 °C)

lustrated in **Fig. 5** ***a***, the boron adsorption attained an equilibrium state after 720 min (12 h). The adsorption reaction exhibited a rapid progression during

Table 2

Boron adsorption capacity of various adsorbents

Adsorbent	q_{max} (mg/g)	Experimental conditions	References
Dowex (XUS 43594.00)	4.28	pH = 8.4	[40]
CM-β-CD-Fe_3O_4NPs	3.98	C_0 = 50 mg/L, pH = 5, 1h, dose = 0.3 g	[9]
Activated carbon	1.30	C_0 = 5—100 mg/L, pH = 9.26, 22 °C, 3h, dose = 1.0 g/100 mL	[13]
Amorphous carbon	1.85		
Raw pomegranate peel powder	0.61	C_0 = 3—20 mg/L, pH = 6, 30 °C, 130 min, dose = 1.0 g/100 mL	[2]
Raw pomegranate peel powder modified with HCl	0.91		
Raw pomegranate peel powder modified with NaOH	0.97		
Crosslinked gluconated chitosan particles	4.13	C_0 = 10—400 mg/L, pH = 5.45, 25 °C, 24h, dose = 0.8 g/20 mL	[31]
Crosslinked gluconated chitosan nanofiber beads	6.05		
Amberlite IRA 743 resin	6.39	C_0 = 10—400 mg/L, pH = 8.02, 25 °C, 24h, dose = 0.8 g/20 mL	Original data
Amberlite IRA 743 resin-AAT	9.75		

the initial period, which can be attributed to the substantial availability of active sites present on the resins. The active sites showed a propensity to saturate as the contact time increased, ultimately resulting in the reaction achieving sorption equilibrium after 12 h.

The implementation of pseudo-first-order, pseudo-second-order, and intra-particle diffusion models to the experimental data is depicted in plots **Fig. 5** ***b—d.*** The value of the correlation coefficients and rate constants is exhibited in Table 3.

The findings revealed that pseudo-first-order and pseudo-second-order models fit the experimental data better than intra-particle diffusion model. Thus, the adsorption kinetics can be explained by pseudo-first-order and pseudo-second-order. Nevertheless, pseudo-second-order is relatively better fitted with higher correlation coefficients R^2 values of 0.9981 and 0.9972 for Amberlite IRA 743 resin-AAT and Amberlite IRA 743 resin, respectively (Table 3). This observation suggests that the ionic interaction between boron and various resins is predominant, indicating that the adsorption process is governed by the chemisorption mechanism.

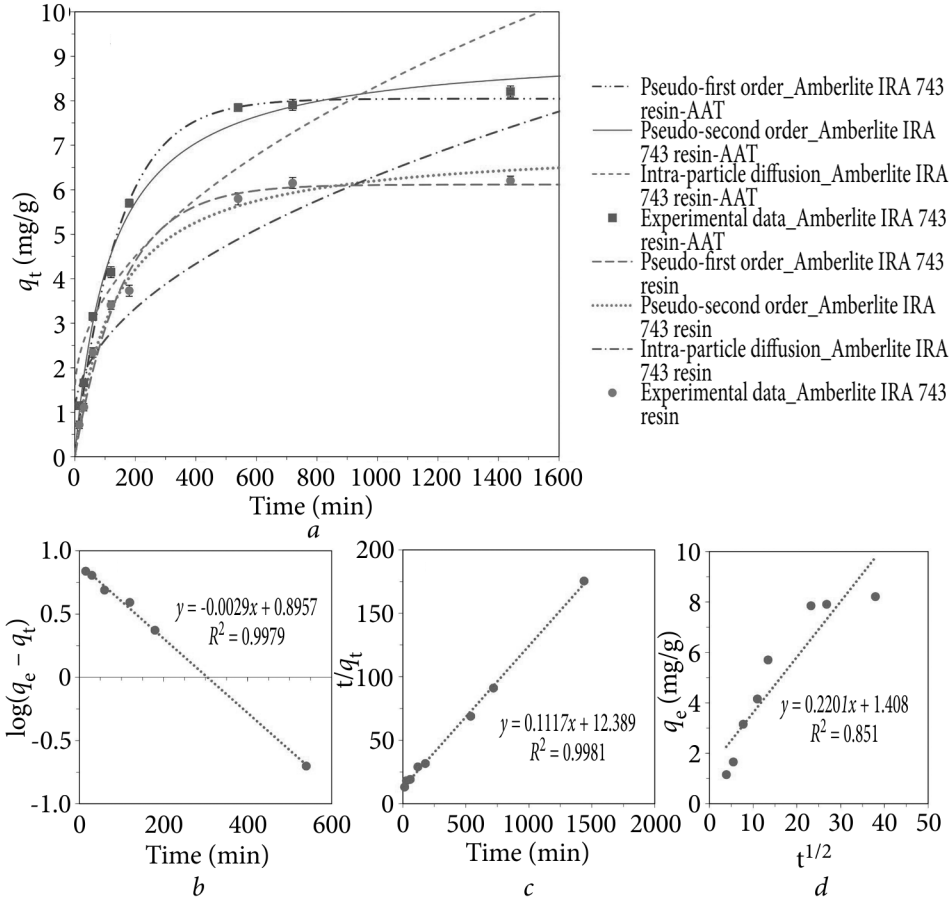

Fig. 5. Pseudo-first order, the pseudo-second order, and intra-particle diffusion models fitting of boron adsorption onto Amberlite IRA 743 resin-AAT and Amberlite IRA 743 resin (*a*); Linear pseudo-first order model of Amberlite IRA 743 resin-AAT (*b*); Linear pseudo-second order model of Amberlite IRA 743 resin-AAT (*c*); Linear intra-particle model of Amberlite IRA 743 resin-AAT (*d*) (initial pH — 8.02, initial boron concentration — 400 mg/L, resin dosage — 0.8 g, solution volume — 20 mL, contact time — 24 h, temperature — 25°C)

The mechanism behind the adsorption of boron by utilizing Amberlite IRA 743 resin and Amberlite IRA 743 resin-AAT is shown in **Fig. 6**. The process of boron adsorption using Amberlite IRA 743 resin, as shown in **Fig. 6, *a***, involves the formation of chemical bonds between the boron species and the hydroxyl functional groups on the adsorbent. The Amberlite IRA 743 resin, which contains hydroxyl-functionalized sites and quaternary amine groups, is particularly suitable for this adsorption process. The interaction between the resin's functional groups and the boron species involves both electrostatic forces and complexity. When boron is present in the solution, it can form complexes with the hydroxyl groups of the resin, leading to the formation of boron-hydroxy complexes that are efficiently adsorbed onto the resin surface.

Table 3

Fitting parameters of pseudo-first order, the pseudo-second order, and intra-particle diffusion models for boron adsorption using Amberlite IRA 743 resin-AAT and Amberlite IRA 743 resin

Adsorbent	Pseudo-first order			Pseudo-second order			Intra-particle diffusion		
	k_1 (min^{-1})	q_{max} (mg/g)	R^2	k_2 (g mg^{-1} min^{-1})	q_{max} (mg/g)	R^2	K_{diff} (mg g^{-1} $min^{-1/2}$)	C (mg g^{-1})	R^2
Amberlite IRA 743 resin	0.0063	6.12± 0.082	0.9949	0.0011	7.04	0.9972	0.1711	0.9126	0.8644
Amberlite IRA 743 resin-AAT	0.0070	8.05± 0.124	0.9979	0.0009	9.21	0.9981	0.2191	1.4062	0.8510

This adsorption is enhanced by the presence of quaternary amine groups on the resin, which can assist in stabilizing the complex formed between the resin and the boron species. For Amberlite IRA 743 resin-AAT, the surface of the resin comprises more negative charge after the treatment process (**Fig. 6, *b***). This increased the interaction between boron species and hydroxyl groups, which improved the boron adsorption capacity. The treatment of resin strongly suggested that Amberlite IRA 743 resin is an effective and versatile material for boron removal from aqueous solutions.

Inorganic salts are commonly present in seawater and surface water, and their existence can influence the effectiveness of boron removal. In order to explore the potential interference caused by salts, the tests were conducted on boron adsorption in the presence of Na^+, K^+, Ca^{2+} and Mg^{2+}, which are prevalent ions in water resources. As illustrated in **Fig. 7**, the presence of foreign ions Na^+ and K^+ does not significantly interfere with the boron sorption capacity of Amberlite IRA 743-AAT resin and Amberlite IRA 743 resin. Conversely, the introduction of Ca^{2+} and Mg^{2+} could enhance the boron adsorption capacity of Amberlite IRA 743-AAT resin and Amberlite IRA 743 resin. This effect is ascribed to two hydroxyl groups bonding to Ca^{2+} and Mg^{2+} ions, which can react with boron to form stable complexes in an aqueous solution. A similar result was observed on boron adsorption of other adsorbents containing *vis*-diols. This suggests that Amberlite IRA 743-AAT resin and Amberlite IRA 743 resin exhibit specific boron removal in the presence of $CaCl_2$ and $MgCl_2$, which are commonly found in seawater.

The recycling and regeneration of the adsorbents is essential for practical applications. Thus, the regeneration capacity

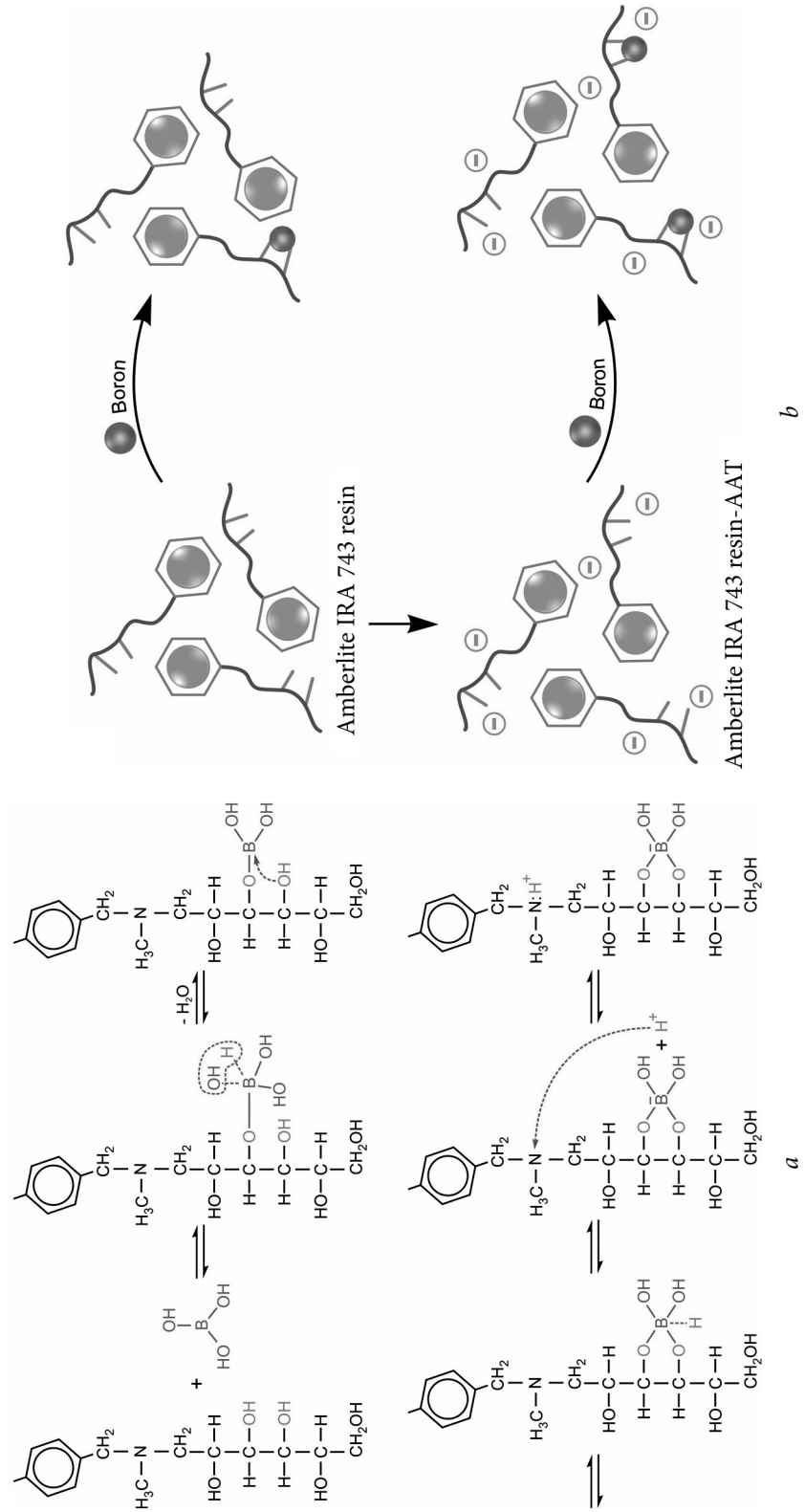

Fig. 6. Possible boron adsorption by Amberlite IRA 743 resin (*a*) and Amberlite IRA 743 resin-AAT (*b*)

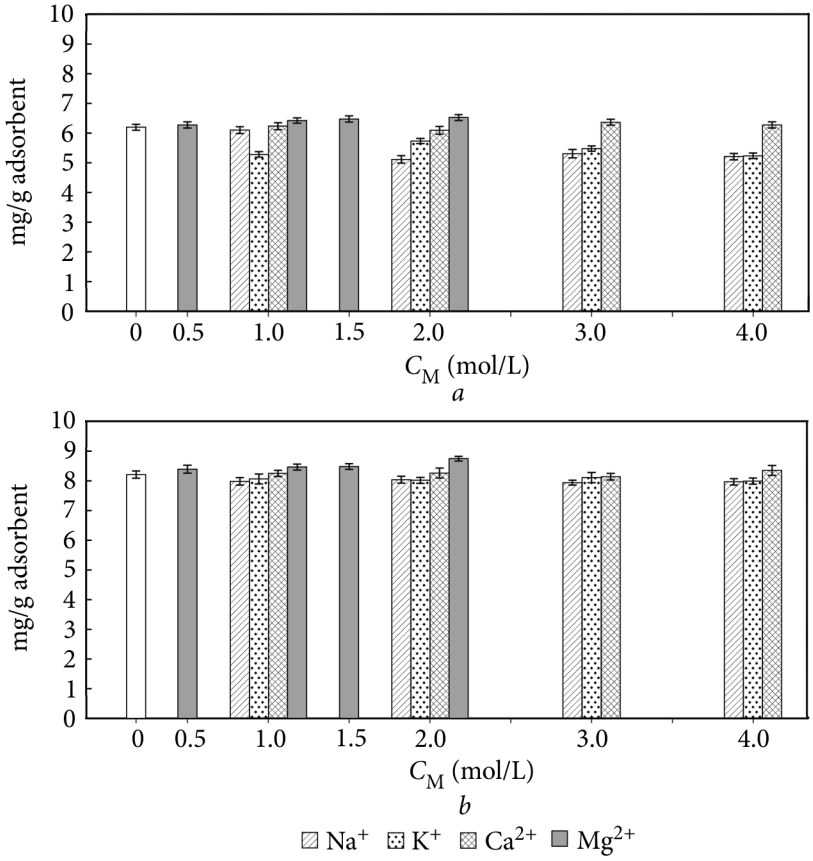

Fig. 7. Effect of the concentration of NaCl, KCl, $CaCl_2$, and $MgCl_2$ on boron adsorption capacity of Amberlite IRA 743 resin (*a*) and Amberlite IRA 743 resin-AAT (*b*)

of Amberlite IRA 743-AAT resin and Amberlite IRA 743 resin was investigated. The influence of pH on boron adsorption for both Amberlite IRA 743-AAT resin and Amberlite IRA 743 resin was examined. The findings demonstrate that a reduction in adsorption capacity was observed at lower pH levels, and the maximum boron adsorption was reached at pH of 8; therefore, adsorbents can be easily regenerated through immersion in acidic solution and subsequently reactivated in alkaline conditions. Amberlite IRA 743-AAT resin and Amberlite IRA 743 resin were washed several times with Mili-Q water. After this step, resins were dipped in 0.1 M HCl solution, rinsed several times with Mili-Q water, and then immersed in 0.1 M NaOH solution for the regeneration process. As shown in **Fig. 8**, the regeneration efficiency of Amberlite IRA 743-AAT resin and Amberlite IRA 743 resin remained 81.9 % and 71.1 % after 6 cycles, respectively. The results indicate that Amberlite IRA 743 resin-AAT can be utilized as a recyclable adsorbent for boron removal.

For application in wastewater, a sample was obtained from wet flue gas desulfurization wastewater of the local coal-fired power plant (Thanh Hoa province, Viet Nam). To eliminate total suspended solids, the wastewater sample

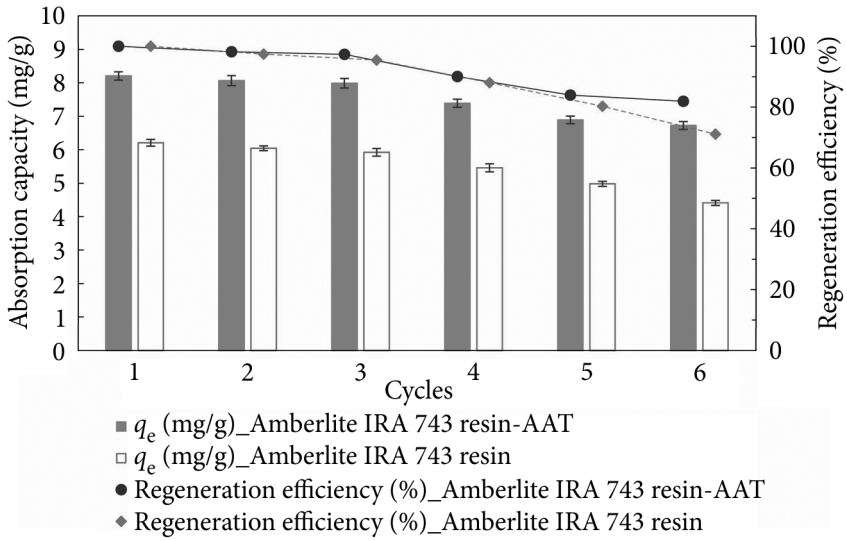

Fig. 8. The reusability of Amberlite IRA 743 resin-AAT and Amberlite IRA 743 resin

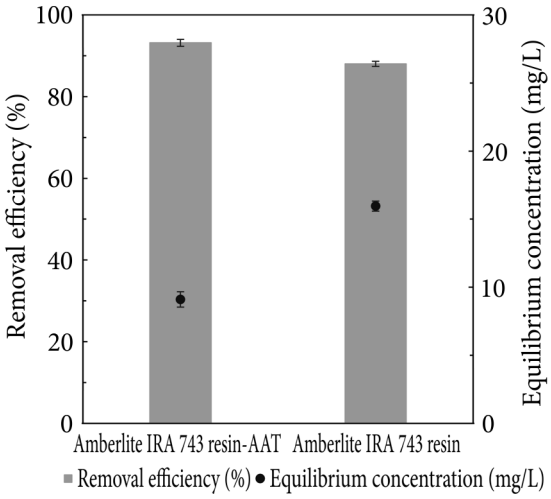

Fig. 9. Boron removal efficiency in the wet flue gas desulfurization wastewater of the local coal-fired power plant using Amberlite IRA 743 resin-AAT and Amberlite IRA 743 resin

Table 4

Properties of flue gas desulfurization wastewater
(concentrations in mg/L)

Parameters	FGD wastewater
pH	6.6
Na^{+}	1261.40
Ca^{2+}	3627.85
Mg^{2+}	1392.50
B^{3+}	133.29
Se^{6+}	850.38
As^{3+}	0.02
Cr^{5+}	0.04
Zn^{2+}	1.49
Cu^{2+}	0.44
Cd^{2+}	0.03
Ni^{2+}	0.15

underwent filtration (0.45 μm pore size). Following this, 0.8 g of Amberlite IRA 743 resin-AAT or Amberlite IRA 743 resin was introduced into 20 mL of wastewater. The sample was shaken at 25єC for 24 h, and boron concentrations were measured using ICP-AES. The parameters of FGD wastewater are presented in Table 4. After boron adsorption, the concentration of boron was reduced from 133.29 mg/L to 9.10 mg/L and 15.96 mg/L using Amberlite IRA 743 re-

sin-AAT and Amberlite IRA 743 resin, respectively. The boron removal efficiency of Amberlite IRA 743 resin-AAT and Amberlite IRA 743 resin was achieved at 93.2 % and 88.0 %, respectively **(Fig. 9).** The results suggest that Amberlite IRA 743 resin-AAT is an effective resin for boron removal from the wastewater of coal-fired power plants.

Conclusion

In conclusion, this work affirms the heightened effectiveness of activated Amberlite IRA 743 resin compared to commercial Amberlite IRA 743 resin for boron removal. Notably, Amberlite IRA 743 resin-AAT demonstrated a remarkable boron removal efficiency of 82.8 %, significantly outperforming the untreated Amberlite IRA 743 resin (60.4 %) with the initial pH of 8.05. The boron removal capacity of Amberlite IRA 743 resin-AAT significantly enhances as the pH level rises, reaching its peak at a pH of 8. The maximum boron adsorption capacity of Amberlite IRA 743 resin-AAT was 9.75 mg/g, compared to 6.39 mg/g for the untreated resin. The boron removal capacity was increased in the presence of $CaCl_2$ and $MgCl_2$. Furthermore, Amberlite IRA 743 resin-AAT presents the regeneration efficiency at 81.9 % after 6 cycles and the boron removal efficiency at 93.2 % for flue gas desulfurization wastewater from the local coal-fired power plant. However, the effect of foreign ions on boron adsorption needs to be investigated in future work to assess comprehensively the boron removal efficiency of Amberlite IRA 743 resin-AAT. All findings suggest that Amberlite IRA 743 resin-AAT is a highly effective material for boron removal, offering a superior and more efficient solution for environmental remediation. Future work should also include statistical analyses to confirm whether the observed differences between test conditions, including resin types and ionic strengths, are statistically significant.

Literature Cited

1. Akdağ, S.,Keyikoğlu, A. Karagunduz et al. 2023. Recent advances in boron species removal and recovery using layered double hydroxides. *Appl. Clay Sci.* **233**: 106814. https://doi.org/https://doi.org/10.1016/j.clay.2023.106814.

2. Al-Badaii, F., K.M. Jansar, N.A.A. Jalil & A.A. Halim. 2024. Sustainable boron removal from aqueous solutions using pomegranate peel adsorbents: A comprehensive study on isotherms, kinetics, and thermodynamics. *Desalin. Water Treat.* **317**: 100045. https://doi.org/10.1016/j.dwt.2024.100045.

3. Alharati, A., Y. Swesi, K. Fiaty & C. Charcosset. 2017. Boron removal in water using a hybrid membrane process of ion exchange resin and microfiltration without continuous resin addition. *J. Water Process Eng.* **17**: 32—39. https://doi.org/10.1016/j.jwpe.2017.03.002.

4. Alharati, A., Y. Swesi, K. Fiaty & C. Charcosset. 2018. Comparison of boron removal by ion-exchange resin in column and hybrid membrane process. *Desalin. Water Treat.* **129**: 34—42. https://doi.org/10.5004/dwt.2018.22805.

5. Çermikli, E., F. Şen, E. Altıok et al. 2020. Performances of novel chelating ion exchange resins for boron and arsenic removal from saline geothermal water using adsorption-membrane filtration hybrid process. *Desalination* **491**: 114504. https://doi.org/10.1016/j.desal.2020.114504.

6. Cheraghi, R., M. Abrishamkar, H.J. Jahromi & F. Hoseini. 2024. Synthesized polyetheretherketone/polyvinylalcohol nanocomposite modified with zinc oxide nanoparticles:

As an effective adsorbent for removal of arsenic (III) ion from wastewater. *Desalin. Water Treat.* **317**: 100008. https://doi.org/10.1016/j.dwt.2024.100008.

7. Choi, P.J., S.J. Im, S. Ryu et al. 2024. Hybrid multi-chamber system for enhanced removal of boron during water treatment/desalination without chemical usage. *J. Membr. Sci.* **694**: 122419. https://doi.org/10.1016/j.memsci.2024.122419.

8. Darwish, N.B., V. Kochkodan & N. Hilal. 2015. Boron removal from water with fractionized Amberlite IRA743 resin. *Desalination* **370**: 1—6. https://doi.org/10.1016/j.desal.2015.05.009.

9. Ghazali, A.A., M. Farzaneh & B. Mombeni Goodajdar. 2023. Synthesised CM-β-CD-Fe3O4NPs: as an environmental friendly and effective adsorbent for elimination of boron from aqueous solutions. *International Journal of Environmental Analytical Chemistry* **103**: 6324—6343. https://doi.org/10.1080/03067319.2021.1953492.

10. Harkness, J.S., B. Sulkin & A. Vengosh. 2016. Evidence for coal ash ponds leaking in the southeastern united states. *Environ. Sci. Technol.* **50**: 6583—6592. https://doi.org/10.1021/acs.est.6b01727.

11. Ho, H.Q. 2019. Synthesis of eco-friendly adsorbents for the removal of contaminants in wastewater. Doctor Thesis. Tokushima.

12. Hung, W.-C., R.S. Horng & C.-H. Tsai. 2022. Effects of process conditions on simultaneous removal and recovery of boron from boron-laden wastewater using improved bipolar membrane electrodialysis (BMED). *J. Water Process Eng.* **47**: 102650. https://doi.org/10.1016/j.jwpe.2022.102650.

13. Jaouadi, M. & A.H. Hamzaoui. 2019. Boron adsorption onto activated carbon and amorphous carbon prepared from sucrose dehydration. *Desalin. Water Treat.* **149**: 150—156. https://doi.org/10.5004/dwt.2019.23890.

14. Jiang, H., Z. Zhao, N. Yu et al. 2023. Synthesis, characterization, and performance comparison of boron using adsorbents based on N-methyl-D-glucosamine. *Chinese Journal of Chemical Engineering* **59**: 16—31. https://doi.org/10.1016/j.cjche.2023.01.012.

15. Kamboh, M.A. & M. Yilmaz. 2013. Synthesis of N-methylglucamine functionalized calix[4]arene based magnetic sporopollenin for the removal of boron from aqueous environment. *Desalination* **310**: 67—74. https://doi.org/10.1016/j.desal.2012.10.034.

16. Ke, Q. & M. Ulbricht. 2022. In situ reactive coating of porous filtration membranes with functional polymer layers to integrate boron adsorber property. *J. Membr. Sci.* **660**: 120851. https://doi.org/https://doi.org/10.1016/j.memsci.2022.120851.

17. Kim, H., S. Kim & C. Kim. 2024. Enhanced boron removal without pre-pH adjustment via redox-mediated electrodialysis assisted by ion-exchange resins. *J. Environ. Chem. Eng.* **12**: 113159. https://doi.org/10.1016/j.jece.2024.113159.

18. Lee, C.-H., P.-H. Chen & W.-S. Chen. 2022. Recovery of boron from desalination brine through Amberlite IRA 743 resin. *DWT* **264**: 133—140. https://doi.org/10.5004/dwt.2022.28569.

19. Li, Y.-F., Y.-J. Liu, C.-H. Yen & C.-Y. Hu. 2023. Boron removal from high sulfate-containing coal-fired power plant wastewater by an ultrasound/bipolar electrocoagulation process with aluminum electrodes. *J. Environ. Chem. Eng.* **11**: 110473. https://doi.org/10.1016/j.jece.2023.110473.

20. Lin, J.-Y. & Y.-H. Huang. 2024. Enhanced boron removal via seed-induced crystal growth of barium perborate in sequential fluidized-bed crystallization. *Chemosphere* **361**: 142569. https://doi.org/10.1016/j.chemosphere.2024.142569.

21. Lin, J.-Y., N.N.N. Mahasti & Y.-H. Huang. 2021. Recent advances in adsorption and coagulation for boron removal from wastewater: A comprehensive review. *J. Hazard. Mater.* **407**: 124401. https://doi.org/10.1016/j.jhazmat.2020.124401.

22. Lyu, Q. & L.-C. Lin. 2024. Rational design of reverse osmosis membranes for boron removal: A counter-intuitive relationship between boron rejection and pore size. *Sep. Purif. Technol.* **331**: 125699. https://doi.org/10.1016/j.seppur.2023.125699.

23. Mahasti, N.N.N., K.-Y. Chang, J.-Y. Lin & Y.-H. Huang. 2024. Multi-stage calcium-based chemical oxo-precipitation application to treat boron-containing flue gas desul-

furization wastewater from coal-fired power plant. *J. Environ. Chem. Eng.* **12**: 113233. https://doi.org/10.1016/j.jece.2024.113233.

24. Mecca, T., M. Ussia, D. Caretti et al. 2020. N-methyl-D-glucamine based cryogels as reusable sponges to enhance heavy metals removal from water. *Chem. Eng. J.* **399**: 125753. https://doi.org/10.1016/j.cej.2020.125753.

25. Meng, X., R. Luo, G. Guo et al. 2022. Boron adsorption and isotopic separation from water by isostructural metal-organic frameworks MIL-100(M). *Desalination* **541**: 116038. https://doi.org/10.1016/j.desal.2022.116038.

26. Moorthy, M.S., D.-J. Seo, H.-J. Song et al. 2013. Magnetic mesoporous silica hybrid nanoparticles for highly selective boron adsorption. *J. Mater. Chem. A* **1**: 12485—12496. https://doi.org/10.1039/C3TA12553J.

27. Najid, N., S. Kouzbour, A. Ruiz-Garcна et al. 2021. Comparison analysis of different technologies for the removal of boron from seawater: A review. *J. Environ. Chem. Eng.* **9**: 105133. https://doi.org/10.1016/j.jece.2021.105133.

28. Niu, J., D. Zhang, J. Shen et al. 2024. Poly (ethylene imine)-mediated dihydroxy-functionalized resin with enhanced adsorption capacity for the extraction of boron from salt lake brine. *J. Environ. Chem. Eng.* **12**: 113779. https://doi.org/10.1016/j.jece.2024.113779.

29. Öcal, Z.B., M.S. Öncel, B. Keskinler et al. 2024. Sustainable treatment of boron industry wastewater with precipitation-adsorption hybrid process and recovery of boron species. *Process. Saf. Environ. Prot.* **182**: 719—726. https://doi.org/10.1016/j.psep.2023.12.006.

30. Palma, P., R. Calderyn, M. Godoy & M.A. Rubio. 2016. Comparative study of two analytical methods to the determination of boron in leachate samples from sanitary landfills and groundwater for routine analysis and feasible on-site environmental monitoring. *International Journal of Environmental Analytical Chemistry* **96**(7): 627—635.

31. Quyen, H.H., H.M. Nguyen, V.C.M. Tran et al. 2025. Hydroxyl-modified chitosan nanofiber beads for sustainable boron removal and environmental applications. *RSC Adv.* **15**: 7090—7102. https://doi.org/10.1039/D5RA00077G.

32. Raval, P., N. Thomas, L. Hamdouna et al. 2023. Boron adsorption kinetics of microcrystalline cellulose and polymer resin. *Langmuir* **39**: 5384—5395. https://doi.org/10.1021/acs.langmuir.3c00021.

33. Rosa, D., D. Cifaldi & L. Di Palma. 2024. Boron removal from wastewater via coordinative adsorption assisted by Fenton-Induced Oxoprecipitation/Flocculation. *Chem. Eng. J.* **498**: 155572. https://doi.org/10.1016/j.cej.2024.155572.

34. Ruhl, L.S., G.S. Dwyer, H. Hsu-Kim et al. 2014. Boron and strontium isotopic characterization of coal combustion residuals: Validation of new environmental tracers. *Environ. Sci. Technol.* **48**: 14790—14798. https://doi.org/10.1021/es503746v.

35. Ruiz-Garcна, A., F.A. Leyn & A. Ramos-Martнn. 2019. Different boron rejection behavior in two RO membranes installed in the same full-scale SWRO desalination plant. *Desalination* **449**: 131—138. https://doi.org/10.1016/j.desal.2018.07.012.

36. Vatankhah, G., F. Parsa, D. Jafari & M. Esfandyari. 2024. Evaluation of adsorptive performance of Mn-doped Fe2O4 nanoparticles loaded on activated carbon in removal of boron ions from synthetic wastewater. *Biomass Convers. Biorefin.* **14**: 26477—26487. https://doi.org/10.1007/s13399-023-04695-8.

37. Wang, X., H. Shao, Z. Chen et al. 2024. PEI grafted defective MOF-808 for enhanced boron removal. *Sep. Purif. Technol.* **336**: 126293. https://doi.org/10.1016/j.seppur.2024.126293.

38. Wu, M.-C., Y.-H. Kao & C.-H. Hou. 2024. Evaluating boron removal from aqueous solutions using membrane capacitive deionization (MCDI): Efficacy and limitations. *J. Environ. Chem. Eng.* **12**: 113104. https://doi.org/10.1016/j.jece.2024.113104.

39. Yao, G., F. Zeng, Z. An et al. 2022. Enhancement mechanism for boron removal at high anodic polarization potential during electrocoagulation using iron-based materials. *J. Environ. Chem. Eng.* **10**: 107279. https://doi.org/10.1016/j.jece.2022.107279.

40. Yılmaz İpek, İ., N. Kabay & M. Yüksel. 2013. Modeling of fixed bed column studies for removal of boron from geothermal water by selective chelating ion exchange resins. *Desalination* **310**: 151—157. https://doi.org/10.1016/j.desal.2012.10.009.

41. Zeytuncu, B., M.E. Pasaoglu, B. Eryildiz et al. 2023. Application of different treatment systems for boron removal from industrial wastewater with extremely high boron content. *J. Water Process Eng.* **55**: 104083. https://doi.org/10.1016/j.jwpe.2023.104083.

Надійшла 4.06.2025

H.H. Quyen,
University of Da Nang, University of Science and Technology,
54 Nguyen Luong Bang Street, Lien Chieu District, Da Nang City 550000, Vietnam
e-mail: hhquyen@dut.udn.vn

H.M. Nguyen,
Department of Aerospace and Mechanical Engineering, University of Notre Dame,
Notre Dame, IN 46556, United States
e-mail: hnguye28@nd.edu

V.C.M. Tran,
University of Da Nang, University of Science and Technology,
54 Nguyen Luong Bang Street, Lien Chieu District, Da Nang City 550000, Vietnam

P.-C. Le,
University of Da Nang, University of Science and Technology,
54 Nguyen Luong Bang Street, Lien Chieu District, Da Nang City 550000, Vietnam

M. Kurashina,
Department of Applied Chemistry, Graduate School of Science and Technology,
Tokushima University, 2-1 Minamijosanjima-cho, Tokushima-shi, Tokushima
770-8506, Japan

M. Yasuzawa,
Department of Applied Chemistry, Graduate School of Science and Technology,
Tokushima University, 2-1 Minamijosanjima-cho, Tokushima-shi, Tokushima
770-8506, Japan

IMPROVING BORON REMOVAL FROM AQUEOUS SOLUTIONS USING AMBERLITE IRA 743 RESIN: THE ROLE OF PH AND RESIN ACTIVATION

Reducing elevated boron levels in aquatic ecosystems is essential due to its toxicity to humans and plants. This study investigates the use of activated Amberlite IRA 743 resin for boron removal from aqueous solutions. Batch experiments examined the effects of pH, initial concentration, contact time, and ionic strength on adsorption. Activation with 0.1 M HCl and 0.1 M NaOH significantly enhanced the adsorption capacity. Boron uptake increased with pH, peaking at pH 8. The Langmuir isotherm fits the data well, with maximum capacities of 6.39 mg/g for untreated and 9.75 mg/g for activated resin. Kinetics followed both pseudo-first- and second-order models, reaching equilibrium at 12 hours. NaCl and KCl had a negligible impact, whereas $CaCl_2$ and $MgCl_2$ improved boron removal. The activated resin achieved up to 93.2 % boron removal in flue gas desulfurization wastewater. These results confirm activated Amberlite IRA 743 resin as a promising adsorbent for boron remediation in contaminated water.

Keywords: *Amberlite IRA743 resin, boron removal, adsorption, activation, adsorption kinetic.*